

NUMERICAL ANALYSIS OF PERFORATED
BUILT-UP OPEN COLD-FORMED STEEL
BEAM

NORADILA BINTI MOHD ALIAS

B. ENG(HONS.) CIVIL ENGINEERING

UNIVERSITI MALAYSIA PAHANG

UNIVERSITI MALAYSIA PAHANG

DECLARATION OF THESIS AND COPYRIGHT

Author's Full Name : NORADILA BINTI MOHD ALIAS

Date of Birth : 22 AUGUST 1994

Title : NUMERICAL ANALYSIS OF PERFORATED BUILT-UP
OPEN COLD-FORMED STEEL BEAM

Academic Session : 2017/2018

I declare that this thesis is classified as:

- CONFIDENTIAL (Contains confidential information under the Official Secret Act 1997)*
- RESTRICTED (Contains restricted information as specified by the organization where research was done)*
- OPEN ACCESS I agree that my thesis to be published as online open access (Full Text)

I acknowledge that Universiti Malaysia Pahang reserves the following rights:

1. The Thesis is the Property of Universiti Malaysia Pahang
2. The Library of Universiti Malaysia Pahang has the right to make copies of the thesis for the purpose of research only.
3. The Library has the right to make copies of the thesis for academic exchange.

Certified by:

(Student's Signature)

(Supervisor's Signature)

NORADILA BINTI MOHD ALIAS
940822085016
Date: 25 JUNE 2018

KHALIMI JOHAN BIN ABD
HAMID
Date: 25 JUNE 2018

NOTE : * If the thesis is CONFIDENTIAL or RESTRICTED, please attach a thesis declaration letter.



SUPERVISOR'S DECLARATION

I hereby declare that I have checked this thesis and in my opinion, this thesis is adequate in terms of scope and quality for the award of the Bachelor Degree of Civil Engineering

(Supervisor's Signature)

Full Name : KHALIMI JOHAN BIN ABD HAMID

Position : LECTURER

Date : 25 June 2018



STUDENT'S DECLARATION

I hereby declare that the work in this thesis is based on my original work except for quotations and citations which have been duly acknowledged. I also declare that it has not been previously or concurrently submitted for any other degree at Universiti Malaysia Pahang or any other institutions.

(Student's Signature)

Full Name : NORADILA BINTI MOHD ALIAS

ID Number : AA14256

Date : 25 June 2018

NUMERICAL ANALYSIS OF PERFORATED BUILT-UP OPEN COLD-
FORMED STEEL BEAM

NORADILA BINTI MOHD ALIAS

Thesis submitted in fulfillment of the requirements
for the award of the
Bachelor Degree in Civil Engineering

Faculty of Civil Engineering and Earth Resources

UNIVERSITI MALAYSIA PAHANG

JUNE 2018

SPECIAL APPRECIATION:

My supportive parents:

**MOHD ALIAS BIN MANSOR
SUPIAH BINTI GHAZALI**

My siblings:

**NORAINI BINTI MOHD ALIAS
NORAINA BINTI MOHD ALIAS
NORALIA BINTI MOHD ALIAS
MUHAMMAD AMIRUL ARIFF BIN MOHD ALIAS**

And all fellow friends. Thank you.

ACKNOWLEDGEMENTS

I honor my humble respectful appreciation and gratitude towards my most graceful and love aspiring merciful Almighty Allah S.W.T for blessing me with all required knowledge, healthy and courage to successfully accomplish and render this final year project as a requirement to graduate in a Bachelor (Hons.) of Civil Engineering from Universiti Malaysia Pahang.

I dedicated my sincere gratitude and appreciations to my final year project supervisor Mr. Khalimi Johan Bin Abd Hamid for giving me an idea and continuous support for my study and research. He was extremely helpful in giving information and guidance that is beneficial for me in writing thesis and learning LUSAS software.

In addition, special thanks to my parents, Mohd Alias Bin Mansor and Supiah Binti Ghazali for a support and advice that encourage me to complete and produce a high quality thesis report. Last but not least, thanks to everyone who involve in this research directly and indirectly.

ABSTRAK

Analisis linear dan analisis linear lengkokan untuk bahagian-bahagian terbuka binaan keluli sejuk tertakluk kepada lenturan telah dikaji. Jumlah 18 rusuk yang mempunyai perbezaan bentuk dan saiz bukaan web diuji di bawah konsep empat titik lenturan dengan kaedah unsur terhingga. Bahagian-bahagian terbuka binaan dipasang dengan skru persendirian daripada dua saluran biasa. Tujuannya adalah untuk mengkaji kesan-kesan bukaan yang mempunyai perbezaan bentuk dan saiz juga untuk mengenalpasti maksimum beban bukin yang boleh ditanggung melalui analisis bukin eigenvalue dan untuk mengenalpasti mod kegagalan bahagian-bahagian terbuka binaan melalui elastik tekanan lenturan. Model unsur terhingga telah dimajukan menggunakan perisian LUSAS 14.0 untuk menganalisa specimen-spesimen yang mempunyai dua perbezaan bentuk bukaan iaitu bulatan dan segiempat sama dengan perbezaan bilangan bukaan dan saiz. Tiga perspektif panjang rusuk yang berbeza; pendek 1000 mm (1), sederhana 1500 mm (2) dan panjang 2000 mm (3). Pin dan roller sebagai sokongan hujung dipasang untuk menjalankan analisa unsur terhingga. Kegagalan setempat disebabkan bentuk dan bilangan bukaan pada plat web bahagian-bahagian binaan terbuka keluli sejuk diperhatikan. Keputusan menunjukkan maksimum beban bukin dan mod kegagalan keluli sejuk berbeza beza dengan kedudukan bukaan.

ABSTRACT

The linear analysis and linear buckling analysis of built-up open sections of cold-formed steel subjected to bending was investigated. A total of 18 beams having different shapes and size of web opening were tested under four point bending by using Finite Element Analysis. The built-up sections were assembled by self-tapping screws from two plain channels. The objectives was to study the effect of perforations having different shapes and sizes together to determine the maximum buckling load that can be carried by eigenvalue bucking analysis and to identify the mode of failure of the sections under elastic bending stress. Finite element model was developed using LUSAS 14.0 software to analyse the specimens having two different shapes of perforation which are circular and square shapes with a different number of opening and sizes. Different length of beam sections used was; short 1000 mm (1), medium 1500 mm (2) and slender 2000 mm (3). Pinned and Roller ended support was assigned to validate the Finite Element Analysis. The localized failure due to the size and number of opening in the web plates of the built-up CFS beam is observed. The results shown the maximum buckling load and the mode of failure of cold-formed steel beam vary with the perforations position.

TABLE OF CONTENT

DECLARATION	
TITLE PAGE	
SPECIAL DEDICATION	ii
ACKNOWLEDGEMENTS	iii
ABSTRAK	iv
ABSTRACT	v
TABLE OF CONTENT	vi
LIST OF TABLES	ix
LIST OF FIGURES	x
LIST OF SYMBOLS	xiii
LIST OF ABBREVIATIONS	xiv
CHAPTER 1 INTRODUCTION	1
1.1 Introduction	1
1.2 Problem Statement	2
1.3 Objectives	3
1.4 Scope of Study	4
1.5 Significant of Study	6
CHAPTER 2 LITERATURE REVIEW	7
2.1 Introduction	7
2.2 Types of Cold-Formed Steel	8
2.3 Applications of Cold-Formed Steel	8

2.4	Built-Up Sections	10
2.4.1	Comparison Built-Up Open & Built-Up Closed	11
2.4.2	Advantages & Disadvantages of Built-Up Section	12
2.5	Experiments on Cold-Formed Steel (CFS) Beams Built-Up Sections with Web Perforations	12
2.6	Elastic Buckling of Cold-Formed Steel (CFS) Beams and Columns with Hole	13
2.7	Finite Element Software	14
CHAPTER 3 METHODOLOGY		15
3.1	Introduction	15
3.2	Review Previous Experimental Works on Beam	18
3.3	Analytical Study From Previous Researcher	18
3.4	Numerical Finite Element Method (LUSAS 14.0)	19
3.5	Finite Element Idealization	19
3.5.1	Modelling	20
3.5.1.1	Beam Modelling	22
3.5.1.2	Joint Modelling	22
3.5.2	Support Boundary and Loading Conditions	23
3.6	Finite Element Analysis	24
4.4.1	Modelling	24
4.4.2	Meshing	28
4.4.3	Geometric	29
4.4.4	Material Properties	31
4.4.1	Joint Modelling	32
4.4.2	Support Condition	34
4.4.3	Loading	36

CHAPTER 4 RESULTS AND DISCUSSION	39
4.1 Introduction	39
4.2 Result of Finite Element Analysis	39
4.3 Linear Analysis	39
4.3.1 Deformed Mesh Square Opening Shapes	40
4.3.2 Deformed Mesh Circular Opening Shapes	44
4.3.3 Contour Stress Square Opening Shapes	48
4.3.4 Contour Stress Circular Opening Shapes	53
4.4 Linear Buckling Analysis (Eigenvalue)	59
4.4.1 Deformed Mesh Square Opening Shapes	59
4.4.2 Deformed Mesh Circular Opening Shapes	63
4.4.3 Contour Stress Square Opening Shapes (Eigenvalue)	68
4.4.4 Contour Stress Circular Opening Shapes (Eigenvalue)	73
CHAPTER 5 CONCLUSION	79
5.1 Introduction	79
5.2 Conclusion	80
REFERENCES	81

LIST OF TABLES

Table 1.1	Parameter of samples	5
Table 2.1	Differences between built-up open section and built-up close section	11
Table 3.1	Specimen modelling simulation by using LUSAS software	21
Table 4.1	Maximum Stress of CFS Beam	58
Table 4.2	Linear Buckling Analysis	78

LIST OF FIGURES

Figure 1.1	Open C-channel and Z-channel steel section	2
Figure 1.2	Built-up sections of CFS (a) Built-up open sections (b) built-up closed sections	3
Figure 1.3	Illustration of BUO-1-2CH cross-section model	4
Figure 2.1	C-section of CFS for purlins at the roof system	9
Figure 2.2	CFS with opening to accommodate piping system	10
Figure 3.1	Flow Chart of the project	17
Figure 3.2	Dimensions of BUO-1-2CH model	20
Figure 3.3	Number of 8 nodes (anticlockwise) for QSL8 element	22
Figure 3.4	Number of 4 nodes for JSH4 joint element	23
Figure 3.5	LUSAS modeler start-up	25
Figure 3.6	Created new file in LUSAS project	25
Figure 3.7	Insert the coordinates	26
Figure 3.8	Modelling C-section frame	26
Figure 3.9	Sweep tools for sweeping structures	27
Figure 3.10	Copy tools for copying functions	27
Figure 3.11	Setting the attribute for mesh	28
Figure 3.12	Surface mesh properties	29
Figure 3.13	Setting the attribute for geometric properties	30
Figure 3.14	Geometric properties Database	30
Figure 3.15	Setting the attribute for material properties	31
Figure 3.16	Database of material properties	31
Figure 3.17	Setting attribute for joint meshing	32
Figure 3.18	Feature mesh selection for joint element	33
Figure 3.19	Detail dataset of joint element	33
Figure 3.20	Setting attribute for support conditions	34
Figure 3.21	Detail dataset for Pinned support	35
Figure 3.22	Detail dataset for Roller XY support	35
Figure 3.23	Setting attribute for loading	36
Figure 3.24	Choose the type of structural loading to be applied	37
Figure 3.25	Insert the 8000 N concentrated load in Y direction	37
Figure 3.26	Completed model of BUO-1-NCH	38
Figure 4.1	Deformed shape for (a) BUO-1-NSH, (b) BUO-1-2SH, (c) BUO-1-4SH	41

Figure 4.2	Deformed shape for (a) BUO-2-NSH, (b) BUO-2-2SH, (c) BUO-2-4SH	42
Figure 4.3	Deformed shape for (a) BUO-3-NSH, (b) BUO-3-2SH, (c) BUO-3-4SH	43
Figure 4.4	Deformed shape for (a) BUO-1-NCH, (b) BUO-1-2CH, (c) BUO-1-4CH	45
Figure 4.5	Deformed shape for (a) BUO-2-NCH, (b) BUO-2-2CH, (c) BUO-2-4CH	46
Figure 4.6	Deformed shape for (a) BUO-3-NCH, (b) BUO-3-2CH, (c) BUO-3-4CH	47
Figure 4.7	Contour stress for (a) BUO-1-NSH, (b) BUO-1-2SH, (c) BUO-1-4SH	49
Figure 4.8	Contour stress for (a) BUO-2-NSH, (b) BUO-2-2SH, (c) BUO-2-4SH	50
Figure 4.9	Contour stress for (a) BUO-3-NSH, (b) BUO-3-2SH, (c) BUO-3-4SH	51
Figure 4.10	Contour stress for (a) BUO-1-NCH, (b) BUO-1-2CH, (c) BUO-1-4CH	54
Figure 4.11	Contour stress for (a) BUO-2-NCH, (b) BUO-2-2CH, (c) BUO-2-4CH	55
Figure 4.12	Contour stress for (a) BUO-3-NCH, (b) BUO-3-2CH, (c) BUO-3-4CH	56
Figure 4.13	Deformed shapes of eigenvalue analysis for (a) BUO-1-NSH, (b) BUO-1-2SH, (c) BUO-1-4SH	60
Figure 4.14	Deformed shapes of eigenvalue analysis for (a) BUO-2-NSH, (b) BUO-2-2SH, (c) BUO-2-4SH	61
Figure 4.15	Deformed shapes of eigenvalue analysis for (a) BUO-3-NSH, (b) BUO-3-2SH, (c) BUO-3-4SH	62
Figure 4.16	Deformed shapes of eigenvalue analysis for (a) BUO-1-NCH, (b) BUO-1-2CH, (c) BUO-1-4CH	64
Figure 4.17	Deformed shapes of eigenvalue analysis for (a) BUO-2-NCH, (b) BUO-2-2CH, (c) BUO-2-4CH	65
Figure 4.18	Deformed shapes of eigenvalue analysis for (a) BUO-3-NCH, (b) BUO-3-2CH, (c) BUO-3-4CH	66
Figure 4.19	Contour stress of eigenvalue analysis for (a) BUO-1-NSH, (b) BUO-1-2SH, (c) BUO-1-4SH	69
Figure 4.20	Contour stress of eigenvalue analysis for (a) BUO-2-NSH, (b) BUO-2-2SH, (c) BUO-2-4SH	70
Figure 4.21	Contour stress of eigenvalue analysis for (a) BUO-3-NSH, (b) BUO-3-2SH, (c) BUO-3-4SH	71

Figure 4.22	Contour stress of eigenvalue analysis for (a) BUO-1-NCH, (b) BUO-1-2CH, (c) BUO-1-4CH	74
Figure 4.23	Contour stress of eigenvalue analysis for (a) BUO-2-NCH, (b) BUO-2-2CH, (c) BUO-2-4CH	75
Figure 4.22	Contour stress of eigenvalue analysis for (a) BUO-3-NCH, (b) BUO-3-2CH, (c) BUO-3-4CH	76

LIST OF SYMBOLS

et al.	And Other
m	Meter (Length Unit)
mm	Millimetre (Length Unit)
N	Newton (Load Unit)
kN	Kilo Newton (Load Unit)
E	Young's Modulus
ν	Poisson Ratio

LIST OF ABBREVIATIONS

CFS	Cold-Formed Steel
FEA	Finite Element Analysis
LUSAS	London University Structural Analysis Software
FEM	Finite Element Modelling
QSL8	Quadrilateral Semi-Loof Curved Thin Shell Elements
JSH4	3D Joint Element

CHAPTER 1

INTRODUCTION

1.1 Introduction

Cold-formed steel (CFS) sections are famous engineered material in residential and commercial construction due to strong, safe, durable and effective cost thus save the construction time. This product is not only provided for construction building but it fulfill the needed for transportation machineries, furniture, equipment, storage rack, facilities and others. CFS is commonly used accredit to its high strength and stiffness, uniformly quality, lightness in weight, economic and non-shrinking at ambient temperatures.

A tremendous diversity of shapes, sizes, and applications based on the requirements of specification are produced by cold forming processes such as folding, press braking and rolling. These processes increase the yield strength and tensile strength of CFS but at the same time decrease the ductility of cold-formed steel sections.

Open sections of CFS such as C-sections and Z-sections (refer Figure 1.1) are extensively used in light steel construction of wall, roof and floor framing members. The main functions of these individual structure framing sections are to carry structural strength, load and stiffness for design purposes.



Figure 1.1 Open C-channel and Z-channel steel section (Source: <https://www.stratco.com.au/our-products/building-construction/steel-framing/>)

1.2 Problem Statement

Perforations are commonly employed at the web of CFS sections to accommodate plumbing, electrical, passage utilities and heating conduits in the wall or ceilings of the buildings. While, in steel storage rack, perforation patterns are provided to allow for shelf configurations. Logically, perforation concept for design can reduce the weight thus, overall cost of project but those perforations will affect the ultimate capacity. The ultimate load capacity decreases with increasing opening sizes and increasing the length of perforation. Therefore, it is a same concept when the opening diameter and opening length increased which relative to web depth, the ultimate strength of CFS will decreased. The buckling behavior not only influenced by reduction of cross-sectional properties but also by the stress concentration that caused by perforation.

As CFS sections, perforated cold-formed steel (PCFS) sections also exhibit a similar failure modes that subjected to compressive and bending loads. The failure modes are including distortional buckling, local buckling and global buckling (torsional).

Various shapes of CFS may have a nice appearance but due to their characteristic which is mono-symmetric such as C-section or Z-section, these open sections are leads to fail under lateral torsional buckling because the location of its centroid and shear center of the cross-section is unsymmetrical. So, both individual sections need to connect each other to form the double-symmetric built-up open sections or built-up close section to have a symmetrical shear center as shown in Figure 1.2 (a) and Figure 1.2 (b). Behavior of CFS as built-up sections need to be observed.

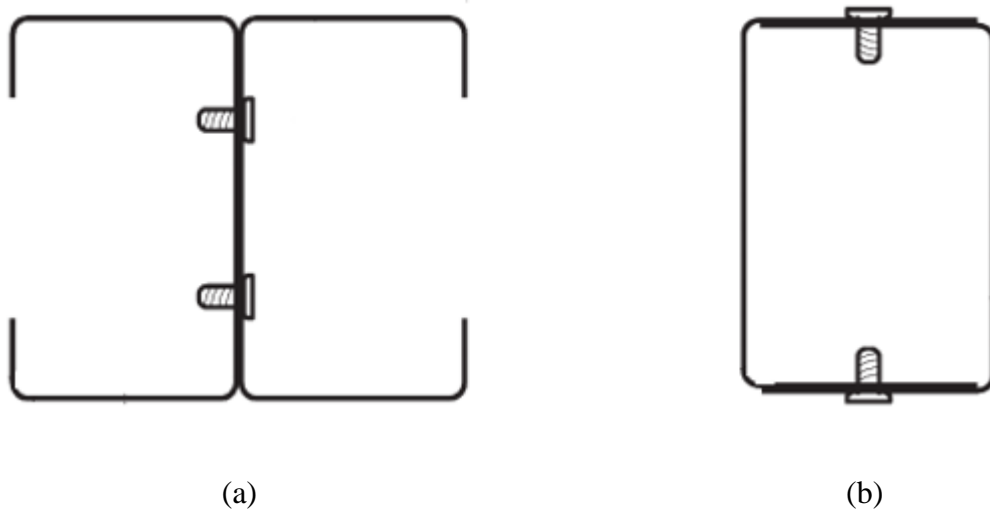


Figure 1.2: Built-up sections of CFS (a) Built-up open sections (b) built-up closed sections (Wang and Young 2015)

1.3 Objectives

The purpose of this research is concerning a Finite Element Analysis (FEA) on the built-up open of perforated CFS sections under bending. Several objectives are listed as follow in order to achieve the research outcomes:

- i) To identify the mode of failure of the sections under bending stress.
- ii) To determine the maximum buckling load that can be carry by open built-up steel section before failure by using eigenvalue buckling analysis.
- iii) To study the effect of different shape and number of perforated CFS open built-up section.

1.4 Scope of Study

The scope of this research covers the analysis of mode of failures of built-up open sections. Two different shapes of perforation which are circular and square shapes are chosen with a different number of openings and three perspectives beam span; short 1000 mm (1), medium 1500 mm (2) and slender 2000 mm (3). The studies will depict that the performance of different length of sections and different shapes and number of perforation will have an effect on stress value of load of CFS built-up sections. The sample is analyzing and illustrative by using Finite Element Modelling (FEM) and Finite Element Analysis (FEA) to gain the outcomes.

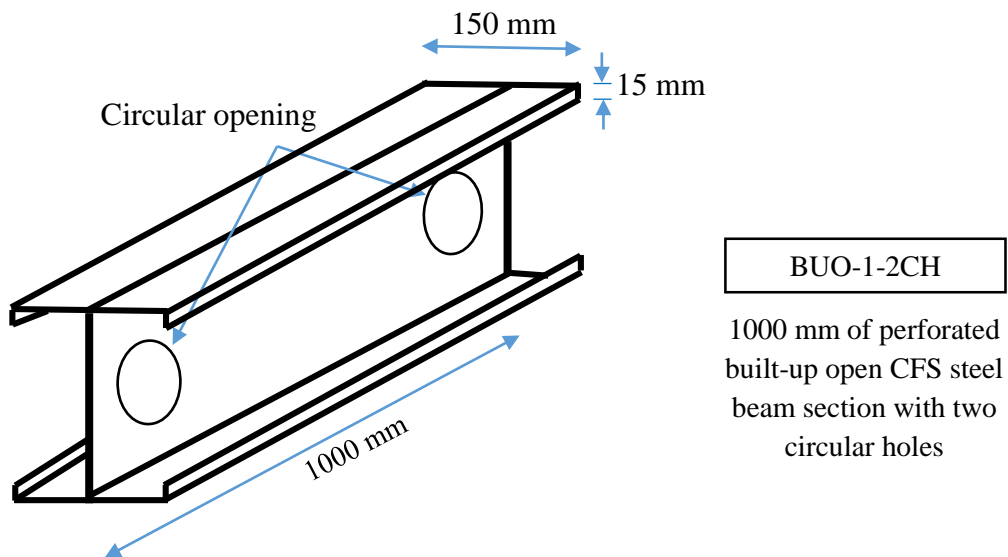

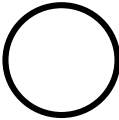
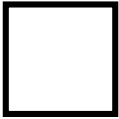


Figure 1.3 Illustration of BUO-1-2CH cross-section model

Table 1.1 Parameters of Specimen

Built-up Open Sections	Shapes Of Opening	Specimen Name	Length (mm)	Number Of Opening
	Circular 	BUO-1-NCH	1000	-
		BUO-1-2CH	1000	2
		BUO-1-4CH	1000	4
		BUO-2-NCH	1500	-
		BUO-2-2CH	1500	2
		BUO-2-4CH	1500	4
		BUO-3-NCH	2000	-
		BUO-3-2CH	2000	2
		BUO-3-4CH	2000	4
	Square 	BUO-1-NSH	1000	-
		BUO-1-2SH	1000	2
		BUO-1-4SH	1000	4
		BUO-2-NSH	1500	-
		BUO-2-2SH	1500	2
		BUO-2-4SH	1500	4
		BUO-3-NSH	2000	-
		BUO-3-2SH	2000	2
		BUO-3-4SH	2000	4

1.5 Significant of Study

The research of perforated CFS built-up sections was carry out by using LUSAS 14.0 Finite Element Analysis (FEA) software. As we know, by creating an opening at the web, it will reduce the weight thus reduce the cost of the steel sections. However, it will exposed to the lack of strength since the original strength of the steel section has been changed due to the perforation. From this simulation analysis, we can determine the ultimate strength of CFS that caused by perforation.

As we know, C-channel steel section tends to face a complicated stress response such as lateral torsional buckling due to mono-symmetric characteristic. So, open built-up steel section was introduced with a double-symmetric characteristic to determine the stress-strain behavior of the steel section. From this numerical investigation, we can identify the failure mode of CFS such as distortional buckling, local buckling and global buckling (torsional).

Finite Element Method (FEM) most prominent due to its inherent generality and numerical efficiency. That's why it is a wider application in industry. The density and configuration of the finite element mesh were determined based on results obtained from convergence studies in order to get more accurate solution besides, minimizing the computational effort (Ling et al., 2015).

Additionally, Finite Element Analysis (FEA)'s main advantage is that it produces a much more detailed set of results than experimental investigations and is often quicker and less expensive. Besides, it required a safe simulation of potentially dangerous, destructive or impractical load conditions and failure modes. The simultaneous calculation and visual representation of a wide variety of physical parameters such as stress or temperature, enabling the designer to rapidly analyze performance and possible modifications. The FEM has widespread adoption for increasingly diverse problems and dominated the market of commercial analysis software (Jim, 2009).

CHAPTER 2

LITERATURE REVIEW

2.1 Introductions

This chapter will describe in detail some of research works conducted by various researchers to design the perforated built-up sections of Cold-Formed Steel (CFS) beam by numerical analysis and experimental practice. Research works is conducted to verified Finite Element (FE) models for built-up sections with opening against the test results that have been carried by the researchers. A review of development of the perforated built-up section of CFS together with the assembling of self-tapping screws can be used as a guidelines to get an appropriate approach in further development to determine the mode of failure by the maximum stresses including the influence of the perforated CFS beam.

CFS is a process of rolling steel into semi-finished at relatively low temperature. The CFS products are created in various shapes that made up by bending sheet or strip steel in roll-forming machines, press brakes or bending brakes. A multiplicity of widely different products, with a tremendous diversity of shapes, sizes, and applications are produced in steel using cold forming processes such as folding, press-braking and rolling (Kulatunga et al., 2013). It is commonly formed in different shapes that designed in mono-symmetric open section such as C-section, U-section, Z-section and also hat-shaped sections which carried a variety functions itself.

2.2 Types of Cold-Formed Steel

In building construction, there are two types of steel structure which are Hot-Rolled Steel (HRS) and CFS (Laboube et al., 2010). HRS shapes are formed at higher temperature while CFS shapes are formed at low temperature. There are two types of CFS commonly used in construction industry which are individual structure framing members and panels and decks. CFS is used for structure framing such as truss, rafters and wall studs (Ye et al., 2016).

Different shape of sections such as C-section, Z-section, I-section, T-section, hat-section and tubular-section are classified as individual structure framing members or sections which typically used in lightweight structure such as joists and purlins due to thin and light behaviour. However, second type of CFS which is panels and decks generally used for floor deck, wall panel, roof decks and others. Typical CFS members such as studs, track, purlins, and grits are mainly used for carrying loads while panels and decks constitute a useful surface such as floor, roof and walls.

2.3 Applications of Cold-Formed Steel

Generally, CFS is used due to its ability to carry structural strength, load and stiffness in the design. Popularity of CFS structure due to lightweight design and economy in transportations and handling has widely applied in buildings automobiles, homes equipment, office furniture, storage racks, highway products, drainage facilities and also bridges. CFS members have been mainly applied to light steel structure and can be used for whole buildings (Kulatunga et al., 2013).

Today, every new structure is created together with a function that can be applied for the real life. As CFS had develop in variety of shapes, it can be propose for variety application. CFS sections such as C and Z sections are commonly used for purlin system (refer Figure 2.1). The sections are commonly installed as purlin system due to lightweight which helps to carry the load from the roof to the bottom of the structures. But, due to thin-walled nature instability phenomena and lack of symmetry (singly-symmetric member), this sections need to be examined in term of failure, local, torsional and global buckling modes. As stated by Vieira et al., 2010, in uplift, the purlins tend to

twist resulting in the addition of longitudinal stresses due to partially restrained warping torsion in addition to conventional bending stress.

CFS is produce with a thin sheet behaviour which able to create a different opening holes at the web. Because of that, CFS is designed not only to cater the loads, but also help to carry an electrics conduits or piping systems (refer Figure 2.2). Holes can be found in most CFS structural components such as in low and midrise construction, evenly-spaced holes are placed in the webs of CFS columns and beams, allowing electrical, plumbing, and heating services to pass through walls and ceilings (Kim et al., 2010).



Figure 2.1 C-section of CFS for purlins at the roof system (Source: <https://mtc-china.com/steel-purlins/>)



Figure 2.2 CFS with opening to accommodate piping system (Source: http://www.steel framing.org/PDF/quicklinks/SFA_Trades_Guide_11-08.pdf)

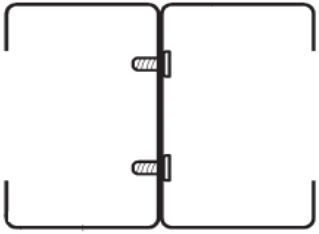
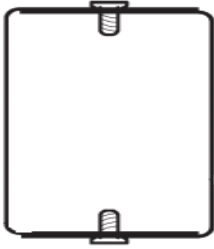
2.4 Built-Up Sections

Mono-symmetric open C-Sections and Z-sections are commonly used especially for light steel construction industry such as floor joist. But, they are created by having an unsymmetrical centroid and shear centre of the cross-section. However, this kind of sections could fail by lateral torsional buckling due to the location of its shear centre and centroid of the cross-section. By connecting two individual sections each other they will formed a double-symmetric built-up open sections or built-up close section that having a symmetrical shear centre. The concept of this built-up sections are referring to the research of beam tests of CFS built-up sections with web perforations by Wang et al., 2015.

2.4.1 Comparison Built-Up Open and Built-Up Close

Built-up open sections and built-up close sections are two combinations of C section which generate a few difference criteria. Table 2.1 below shows the differences between built-up open section and built-up close section:

Table 2.1 Differences between built-up open section and built-up close section

Built-Up Open Section		Built-Up Close Section
	Types of built-up	
Web of built-up sections		Location of Connector
Have lip for C section	Lip	Do not have lip for C-section
Back-to-back	Built-up method	Face-to-face

2.4.2 Advantages & Disadvantages of Built-Up Section

Advantages of Built-up sections:

- i) More versatile since you are not limited to the shapes in the catalogue
- ii) These could be produced in a built-up form much more quickly and potentially contributing better to the domestic economy

Disadvantages of Built-up sections:

- i) Buckling resistance of the high-strength steel affected by residual stress on the cross-section
- ii) Due to the relatively poor torsional performance, it lead to reverse when flexural compression occur
- iii) some shapes are not produced very often or may need to be shipped from overseas and may take too long to arrive to meet the schedule for a project

2.5 Experiments on Cold-Formed Steel (CFS) Beams Built-Up Sections with Web Perforation

CFS structural member such as C and Z sections are commonly provided with perforations to accommodate plumbing, electrical conduit and piping system in the buildings. These perforations are typically pre-punched perforations located at the web of the sections and help to alter the elastic stiffness and ultimate strength of member.

The objectives of the paper conducted by Wang et al., 2015 is to investigate the flexural behaviour, the ultimate moment capacities and failure modes of built-up CFS members with circular web holes. The specimens were assembled by self-tapping screws from two plain channels or lipped channels. Different holes diameter with ten cross-section sizes of 43 simply supported beams specimen were tested under four-point bending.

Different approaches of determining the critical elastic local and distortional buckling moments including the influence of holes for the built-up open and closed sections were compared and discussed. It found that when the holes diameter-to-web depth ratio increases from 0.25 to 0.5, the reduction of ultimate moments is very small with a maximum value of 6%. When the value further increases from 0.25 to 0.7, maximum reduction moment capacities of beams is up to 16%. The presence of web holes was also found to initiate the failure for all built-up section beams in the test.

However, the research paper by Wang et al., 2017 is to carry out the same objectives but by numerical investigation of Finite Element Analysis (FEA) and experimental result of Direct Strength Method (DSM).

2.6 Elastic Buckling of Cold-Formed Steel (CFS) Beams and Columns with Holes

The studies on structural behaviour of CFS is the most popular field due to its interesting failure modes for approximating the local, distortional and global buckling load. Local buckling involves a change in cross-sectional shape and includes only rotation, not translation at the fold lines (Gilbert et al., 2012). Distortional buckling which is known as local torsional buckling or stiffener buckling. It usually involves rotation of the flange in members with the edge stiffed elements. Global buckling is a combination of bending and twisting response of a member in compression. The strength and efficiency of CFS profile depend on the cross-sectional shape which controls the three functional buckling modes: local, distortional and global (Gilbert et al., 2012).

2.7 Finite Element Software

Finite Element Analysis (FEA) is very modern computational tool. The purpose of FEA software is to reduce the number of prototypes and experiments that have to be run when designing, optimizing and controlling a device or process (LUSAS, 2017). This method has been used successfully to solve very complex structural engineering problems (Malike and Abd Hamid, 2012). It also famous method used in thermal analysis, fluid mechanics and electromagnetic fields. Since the method involves a large number of computations, the uses of the computer to solve a problem is really needed.

In FEA, the continuum is idealized as a structure consisting of a number of individual elements connected only at nodal points. Famous FEA software used by previous researchers are LUSAS, ANSYS and ABAQUS. While saving the time, all the FEA software help to predicted the conditions of the numerous steel, reinforced concrete and combination models. It has been applied to numerous problems and this method has a number of advantages (Altan and Kartal, 2009):

- i) Model irregularly shaped bodies easily
- ii) Handle general load conditions without difficulty
- iii) Vary the size of the element
- iv) Include dynamic effects
- v) Handle non-linear behaviour

LUSAS Modeller 14.0 is a completed software to use for global analysis for all types of structures such as buildings, dams, tunnels, storage tanks and others. This software is been used in this research since it can solve all types of linear, non-linear stress, dynamics, composite and thermal engineering analysis problem, across a range of engineering industries. The simplified method is developed as convenient alternative to accommodate the range of opening shapes, locations and common spacing of specimens in industry.

CHAPTER 3

METHODOLOGY

3.1 Introduction

This chapter describes the analytical procedures proposed for Finite Element Analysis (FEA) of CFS built-up sections with web perforations subjected to bending. The modelling is based on a three-dimensional isotropic finite element approach. Different finite element software of built-up CFS such as ABAQUS, LUSAS and ANSYS have been done by a number of researchers. LUSAS 14.0 which is finite element software has been exploited to conduct the analysis of this research. Methods proposed by previous researchers (Yu, 2012; Wang et al. 2015 and 2017) on the behaviour of CFS beam with perforations were adopted in accordance to the guidance for this study.

As described earlier, mono-symmetric CFS section which is C-sections is connected both individual sections together to form the double-symmetric built-up open sections. These two individual sections are interconnected to each other by means of self-tapping, self-drilling screws. In the proposed finite element model, the built-up open section is modelled as isotropic elements. The theoretical modelling of these connectors is important to predict the structural behaviour of the system. A single type of element namely as ‘joint’ element is proposed to model the connectors.

The reliability of the results obtained from the proposed models developed are checked by comparing them with previous results obtained from both experimental and other theoretical solutions (Yu, 2012; Wang et al. 2015 and 2017).

The scopes of analytical study that will be discussed in this chapter are:

- (a) Different length of built-up open section of beam
- (b) Different shapes and sizes of perforation
- (c) Different numbers of web opening

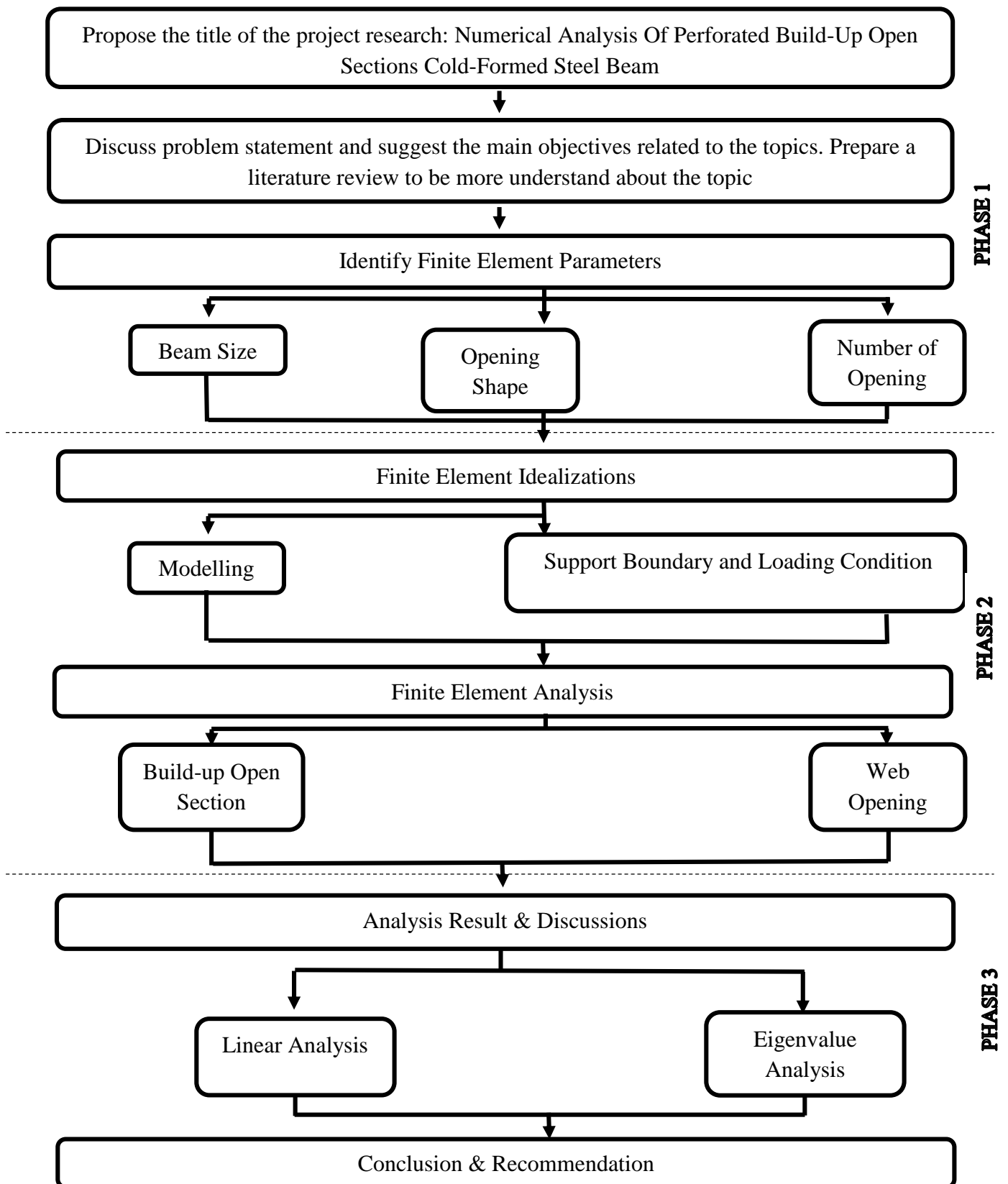


Figure 3.1 Flow Chart of the project

3.2 Review Previous Experimental Works on Beam

It has been mentioned earlier that Wang et al. (2017) has studied the flexural behaviour including the ultimate moment capacities and failure modes of CFS built-up sections with circular web holes. A total of 43 beams having ten cross-section sizes with different hole diameters were tested under four-point bending.

The experimental ultimate moments and corresponding failure modes for CFS built-up open and closed section are summarized. The reduction factor of moment capacity each specimen due to the holes was calculated using the specimen with the holes diameter-to-web depth ratio.

3.3 Analytical Study from Previous Researcher

Finite Element Analysis (FEA) was performed on a wide range of built-up CFS beams with different sizes of perforations under four-point bending. The built-up sections included both I-shaped open sections assembled from two lipped C-channels back-to-back and box-shaped closed sections assembled from two plain channels face-to-face.

Finite element (FE) models have been developed to simulate the simply supported CFS built-up beam sections. The FE model for the 42 built-up open sections and 42 built-up closed sections were verified against the test results that have been conducted by the authors. The validated models were employed to carry out extensive parametric studies on CFS built-up beam sections with various slenderness and holes size.

The beam strengths obtained from the numerical analysis together with the available test data were designed with the design strengths calculated from the current direct strength method (DSM).

3.4 Numerical Finite Element Method (LUSAS 14.0)

In recent years, the FEM has become widely accepted by the engineering professional as an extremely valuable method of analysis. Its application helps the researchers to identify a variety problems with many satisfactory solutions. This FEM will consider the application of the LUSAS finite element package (LUSAS Version 14, 2009) for the analysis of CFS built-up open beam sections with perforation. LUSAS pre-processing options support on screen-modelling and offer excellent options which model a typical section of the structure and the by mirroring, translation and rotation carried out about an axis or a plane to generate the entire structure. The post-processing options include colour plots of strain-stress contours, the deformed shape of the model define by three-dimensional displacement.

3.5 Finite Element Idealization

Finite Element idealization required a procedure to create a finite element model by using LUSAS 14.0 software. The finite element software has been successfully used by many researcher and has proven to be a very effective tool for analysis for steel member and predicting their strength and behaviour (Degtyarev and Degtyareva, 2016). It involves creating a geometric representation of structure and assigning properties then continue with output information in data file. A model is a graphical representation consists of Geometry (Point, Lines, Combined Lines, Surfaces and Volumes) and Attributes (Mesh, Materials, Supports, Loading, etc.).

Finite element idealization is separated into two processes:

- Modelling
- Support Boundary and Loading Condition

3.5.1 Modelling

Finite element software LUSAS 14.0 used to carry out the numerical simulations. The specimen's dimension of 1000 mm beam length of CFS built-up sections with two circular opening is shown in Figure 3.2. Quadrilateral Semi-loof Curved Thin Shell QSL8 with four bending points employed to model all components of a typical lipped C-channel section before it is emulated to become a doubled open (built-up open) section. The material properties of finite element model are same for all sample. In this simulation, linear elastic properties of materials is taken as 210 GPa for Young's Modulus and Poisson's ratio was set to 0.3. The following variables in Table 3.1 are studied:

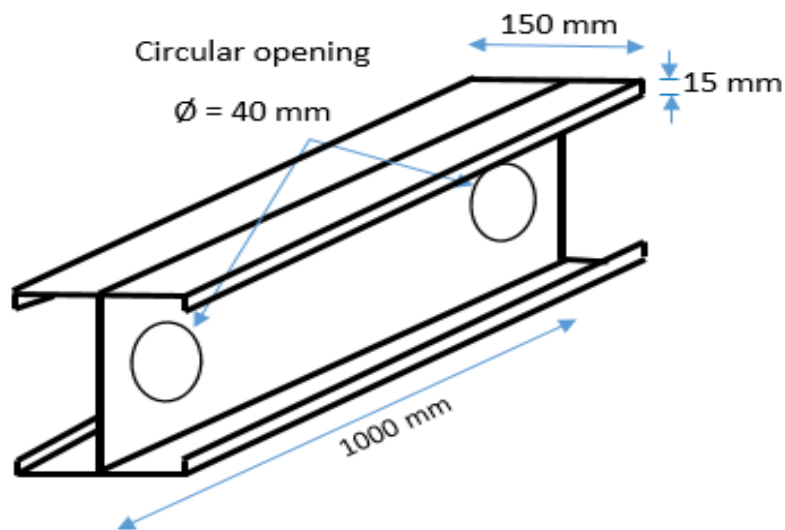
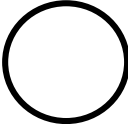



Figure 3.2 Dimensions of BUO-1-2CH model

Table 3.1 Specimen modelling simulation by using LUSAS software

Opening shapes	Opening Sizes (mm)	Beam Length, mm (Number)	Test 1: No Holes	Test 2: Two Holes	Test 3: Four Holes
Circular 	Ø = 40	1000 (1)	BUO-1-NCH	BUO-1-2CH	BUO-1-4CH
	Ø = 50	1500 (2)	BUO-2-NCH	BUO-2-2CH	BUO-2-4CH
	Ø = 60	2000 (3)	BUO-3-NCH	BUO-3-2CH	BUO-3-4CH
Square 	40 x 40	1000 (1)	BUO-1-NSH	BUO-1-2SH	BUO-1-4SH
	50 x 50	1500 (2)	BUO-2-NSH	BUO-2-2SH	BUO-2-4SH
	60 x 60	2000 (3)	BUO-3-NSH	BUO-3-2SH	BUO-3-4SH

3.5.1.1 Beam modelling

In modelling of CFS, it is important to sketch the coordinates of the steel beam C-sections before mirroring to the other side to build it up. Shell element shape is required for meshing aspect of CFS by using Quadrilateral Semi-loof Curved Thin Shell Element, QSL8. Figure 3.3 show the detailed of QSL8 meshing properties. It is a family of shell elements for the analysis of arbitrary curved shell geometries, including multiple branched junctions. The elements can accommodate generally curved geometry with varying thickness and anisotropic and composite material properties. The element formulation takes account of both membrane and flexural deformations. As required by thin shell theory, transverse shearing deformations are excluded.

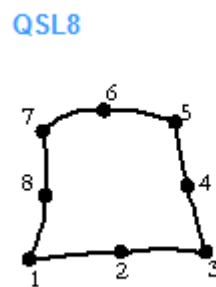


Figure 3.3 Number of 8 nodes (anticlockwise) for QSL8 element (Source: LUSAS, 2009)

3.5.1.2 Joint modelling

The screwed connections between open build-up sections act as a shear connector and mainly shear transferred by shear connector. In this modelling, the screw connections are replaced by 3D joint elements which is JSH4 (refer Figure 3.4). JSH4 is a 3D joint elements that connects two nodes by six springs in the local x, y and z-directions. It has four numbers of nodes which the 3rd and the 4th nodes used to define the local x-axis and local xy-plane respectively. The geometric properties of JSH4 is the eccentricity

measured from the joint xy-plane to nodal line and set as zero. The material properties of joint type is set as general properties for linear joint models which is full joint properties of spring stiffness, mass, coefficient of linear expansion and damping factor. Elastic spring stiffness and mass considered as 625 N/mm^2 , the maximum limit value of joint tensile test.

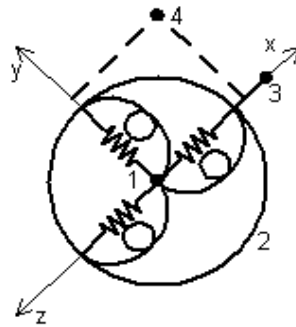


Figure 3.4 Number of 4 nodes for JSH4 joint element (Source: LUSAS, 2009)

3.5.2 Support Boundary and Loading Conditions

Two point load (concentrated load) is located along the flange line at top part of the built-up flange in vertical y-axis negative direction and the load is stated as -8 kN each. Right and left side of the CFS beam is supported by pinned and roller support. In LUSAS 14.0, for pinned support all axis which is x, y and z is assumed as fixed while for roller support, x and y axis is assumed as fixed and z axis is free (Roller XY).

3.6 Finite Element Analysis

Finite Element Analysis (FEA) is emerged to solve any problem of mathematical physics and engineering that related to civil engineering especially in the term to predict the failure of the structure element. FEA software help to moderate the number of prototypes and experiments that need to be run for designing, optimizing, or controlling a process. The finite element method has been successfully used by many research and has proven to be a very effective tool for analysis of steel member and predicting their strength and behaviour (Degtyarev and Degtyareva, 2016). Stages for FEA is shown below:

3.6.1 Modelling

Click a LUSAS Modeller Start-up to create a new model (refer Figure 3.5). Created a new file with a title name. Choose the unit and the vertical axis set as Y direction for the project as shows in Figure 3.6.

Insert the coordinate point (refer Figure 3.7) to define the line representing the shape of structure frame. Click OK to generate the model frame. The model frame single C-sections is illustrate in Figure 3.8.

The surface structure is created using define tools such as “copy”, “sweep”, “move” and others related function. The table properties for sweeping tools of surface structure is show in Figure 3.9. While, Figure 3.10 show the table properties for copy tools.

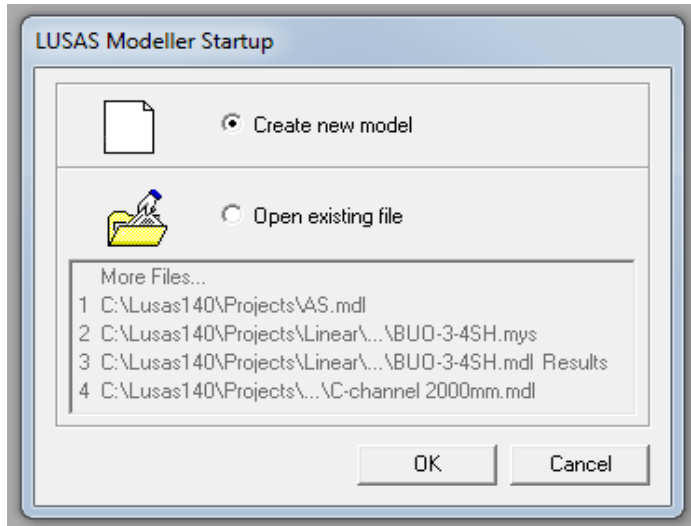


Figure 3.5 LUSAS modeller start-up

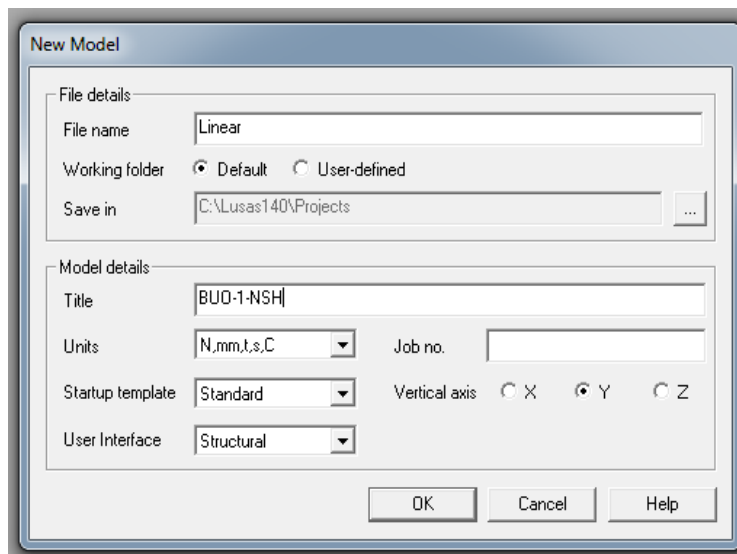


Figure 3.6 Created new file in LUSAS project

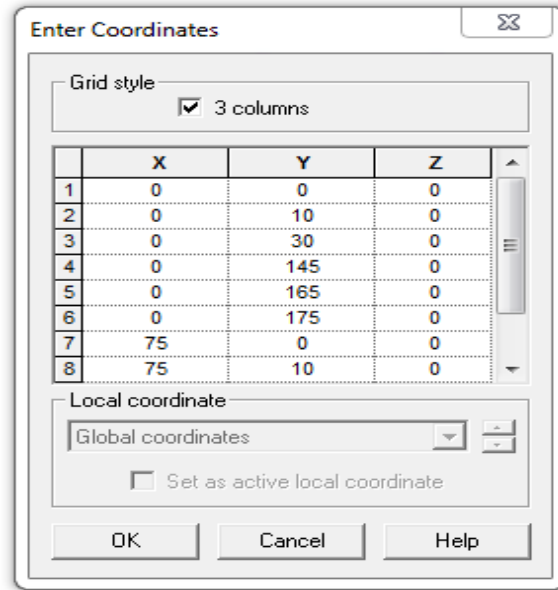


Figure 3.7 Insert the coordinates

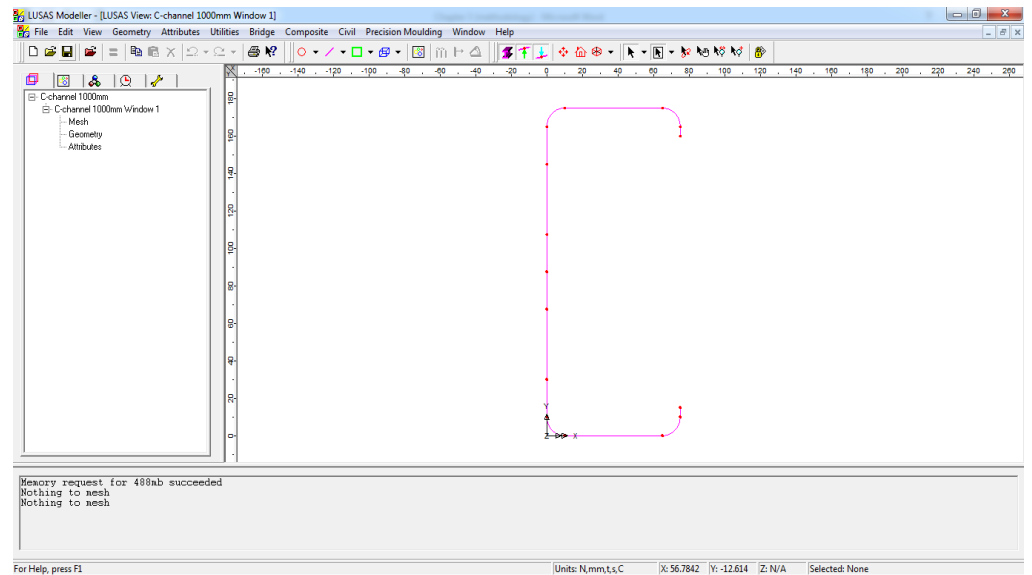


Figure 3.8 Modelling C-section frame

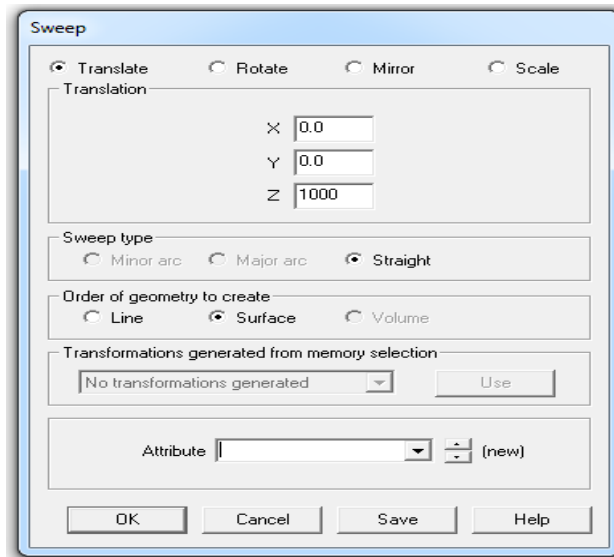


Figure 3.9 Sweep tools for sweeping the structure

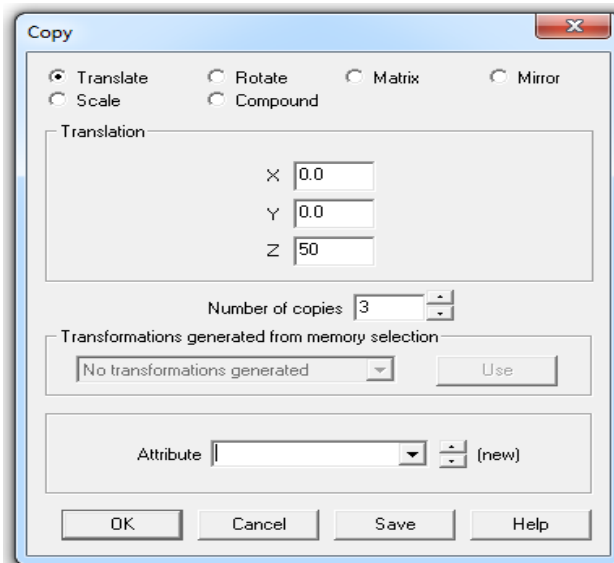


Figure 3.10 Copy tools for copying functions

3.6.2 Meshing

In Figure 3.11, the attributes tab is clicked. Mesh attribute of surface is selected. Insert the element name as QSL8 which is Thin Shell, Quadrilateral element with Quadratic interpolation together with the attribute name and element size as illustrate in Figure 3.12. Click OK to finish then, select the overall model and drag the mesh attribute of QSL8 from the Treeview to the surface model.

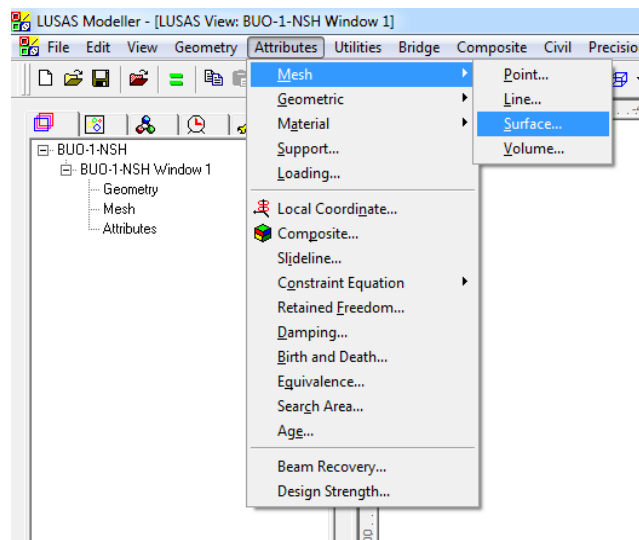


Figure 3.11 Setting the attribute for mesh

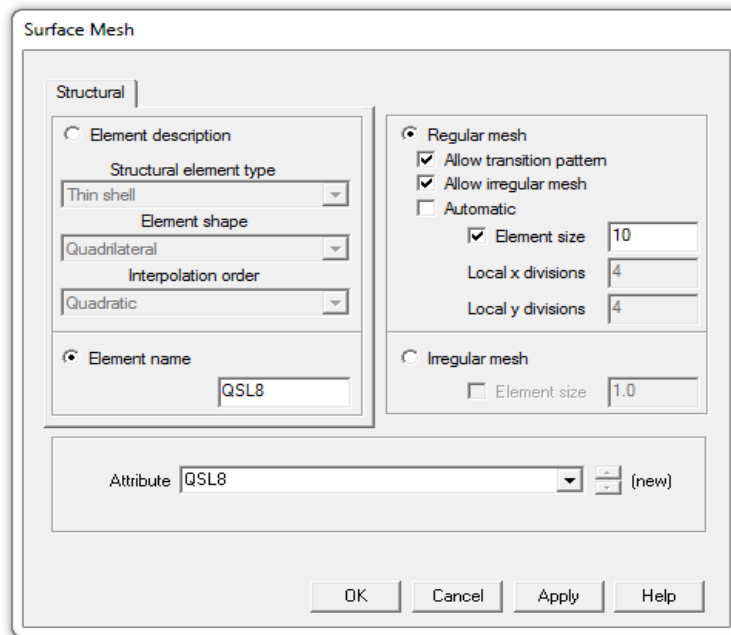


Figure 3.12 Surface mesh properties

3.6.3 Geometric

Click the attributes tab, select geometric then, surface (refer Figure 3.13). Insert the value of thickness as 1.5 mm and eccentricity as zero then, write the attribute name as Thickness = 1.5 mm as show in Figure 3.14. Click OK button to finish. Select the whole model and drag the geometry attributes from Treeview into surface model.

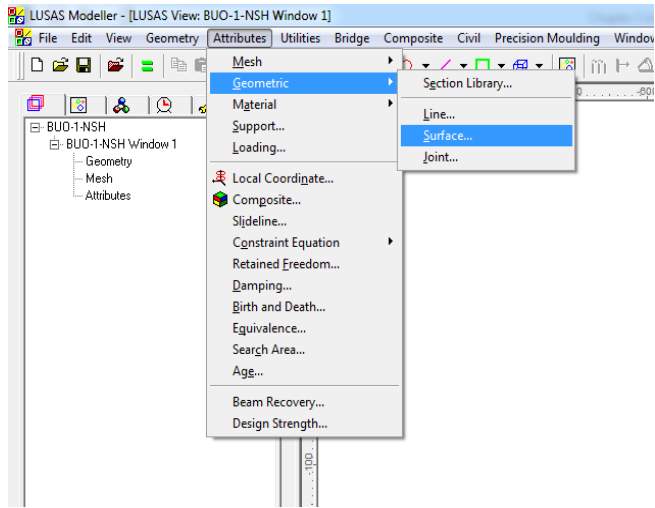


Figure 3.13 Setting the attribute for geometric properties

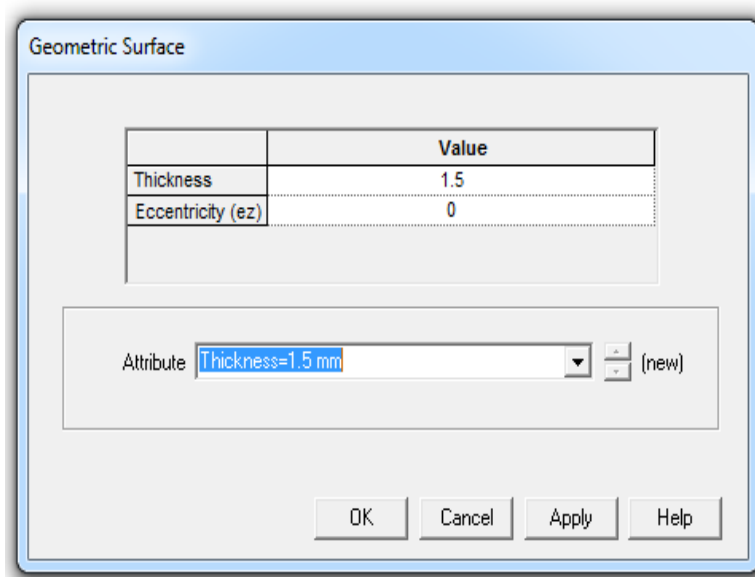


Figure 3.14 Geometric properties database

3.6.4 Material Properties

Click the attributes tab, select material and material library (refer Figure 3.15). Select the Mild Steel as material type with ungraded grade and set the correct units as show in Figure 3.16. Click OK to finish the material properties attribute. Select whole model and drag the geometry attributes from Treeview into surface model.

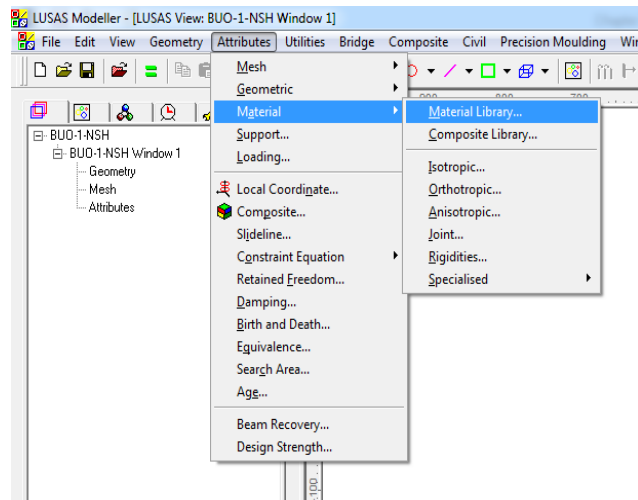


Figure 3.15 Setting the attribute for material properties

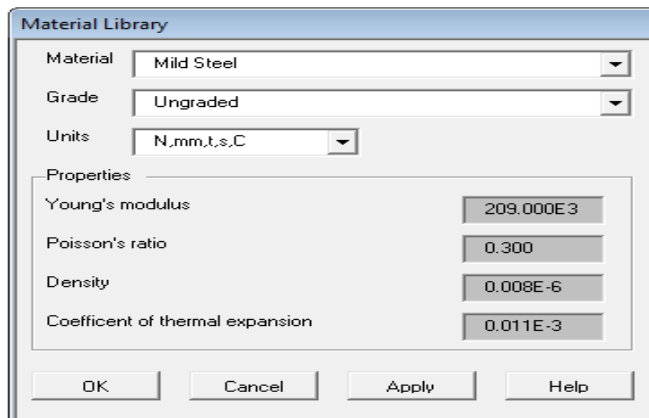


Figure 3.16 Dataset of material properties

3.6.5 Joint Modelling

Click the attributes tab, select mesh and point (refer Figure 3.17). As show in Figure 3.18, select on point mass or joint. Then, click next. Set attribute name and element name as JSH4 with structural element type as joint for beams and 3 dimensional dimension as illustrate in Figure 3.19. Click Finish. Select joint by master to slave from model and drag the joint attribute from Treeview to assign the joint element.

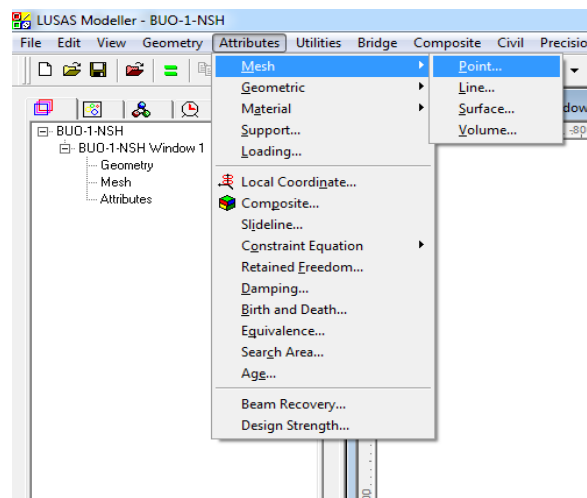


Figure 3.17 Setting attribute for joint meshing

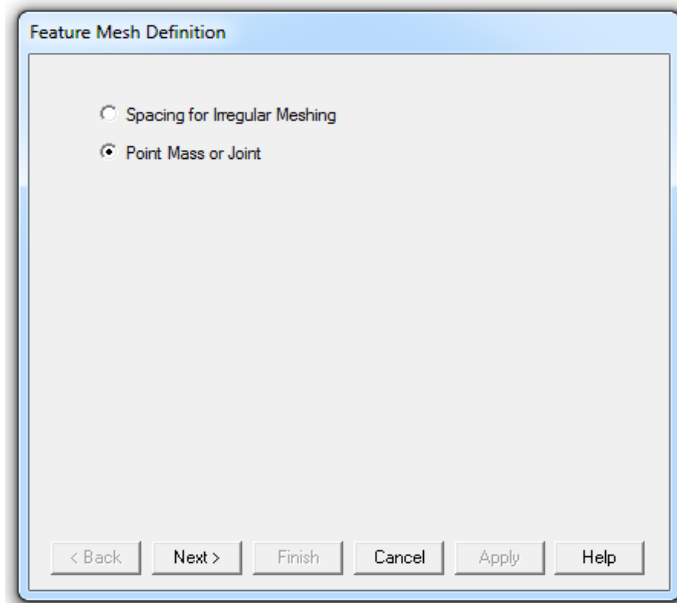


Figure 3.18 Feature mesh selection for joint element

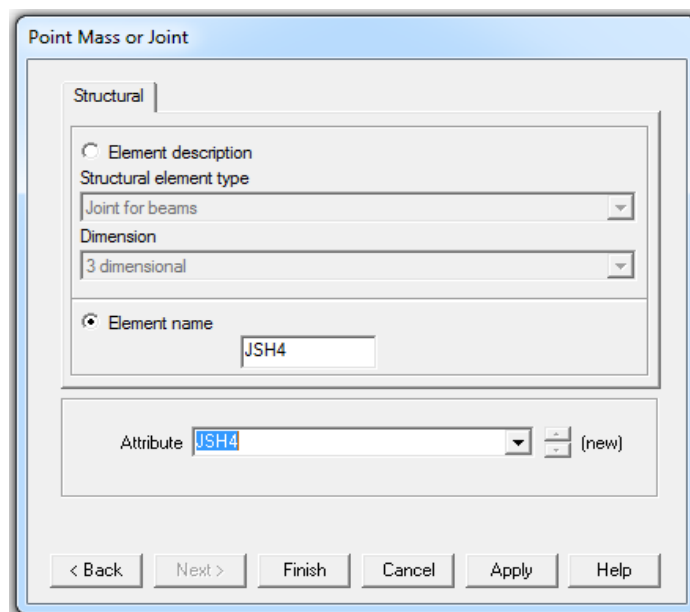


Figure 3.19 Detail dataset of joint element

3.6.6 Support Condition

Click the attributes tab and select support (refer Figure 3.20). Set the translation fixed in the X, Y and Z direction and enter the attribute name as Pinned as show in Figure 3.21. After that, click apply. Set the translation in X and Y directions as fixed and in Z direction as free then, enter the attribute name as Roller XY as illustrate by Figure 3.22. Click OK to finish. Select the lines which represent each support. Drag the support attribute from the Treeview and choose assign to lines.

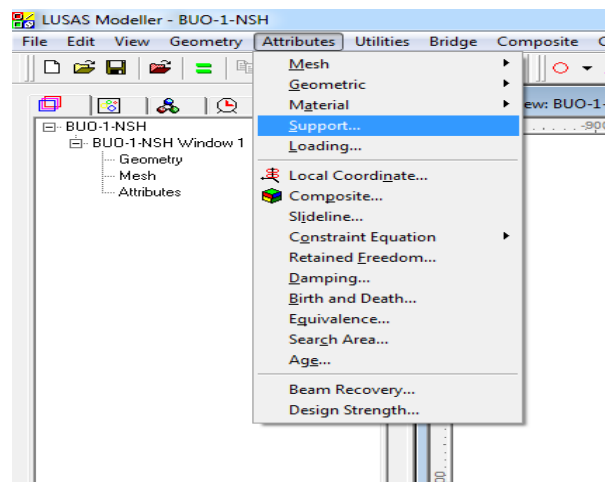


Figure 3.20 Setting attribute for support conditions

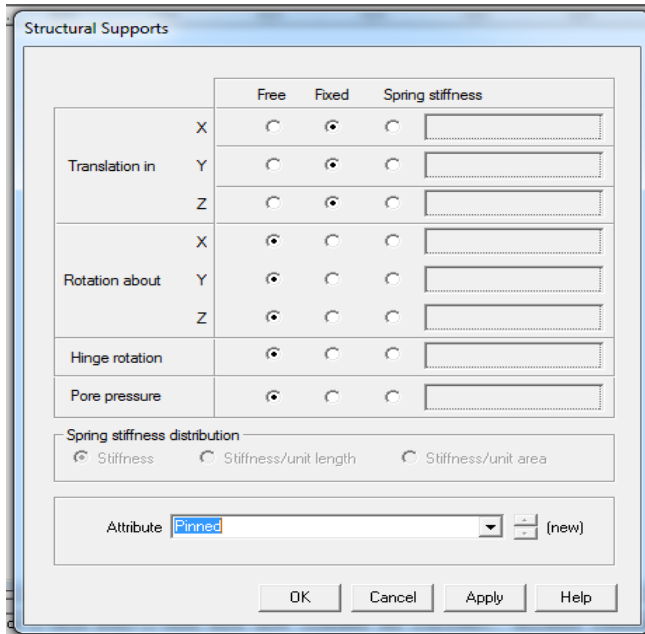


Figure 3.21 Detail dataset for Pinned support

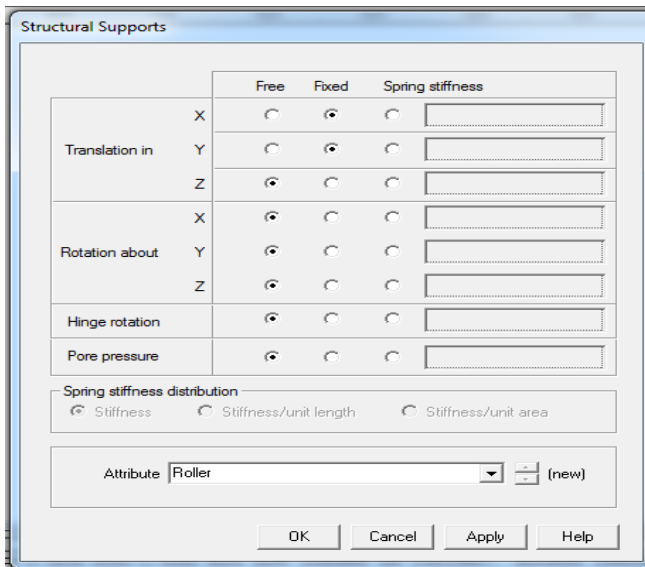


Figure 3.22 Detail dataset for Roller XY support

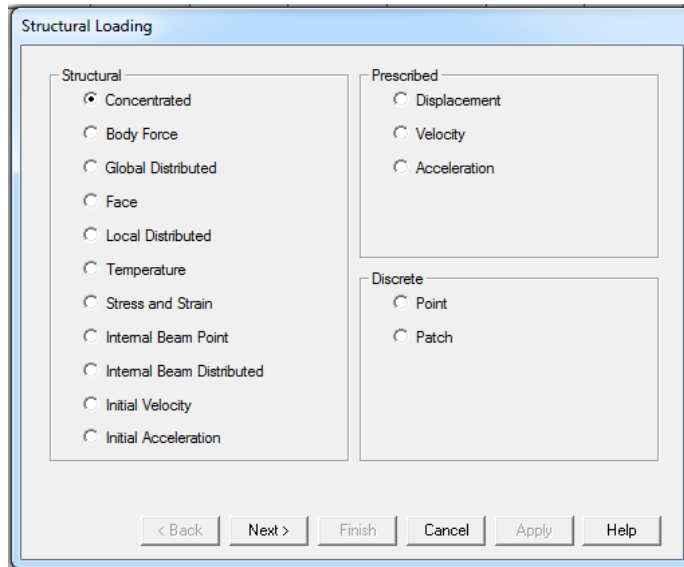


Figure 3.24 Choose the type of structural loading to be applied

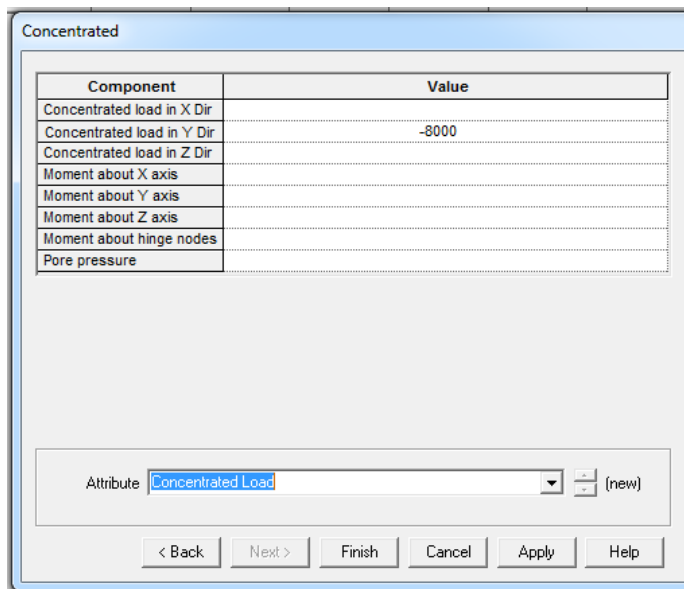


Figure 3.25 Insert the 8000 N concentrated load in Y direction

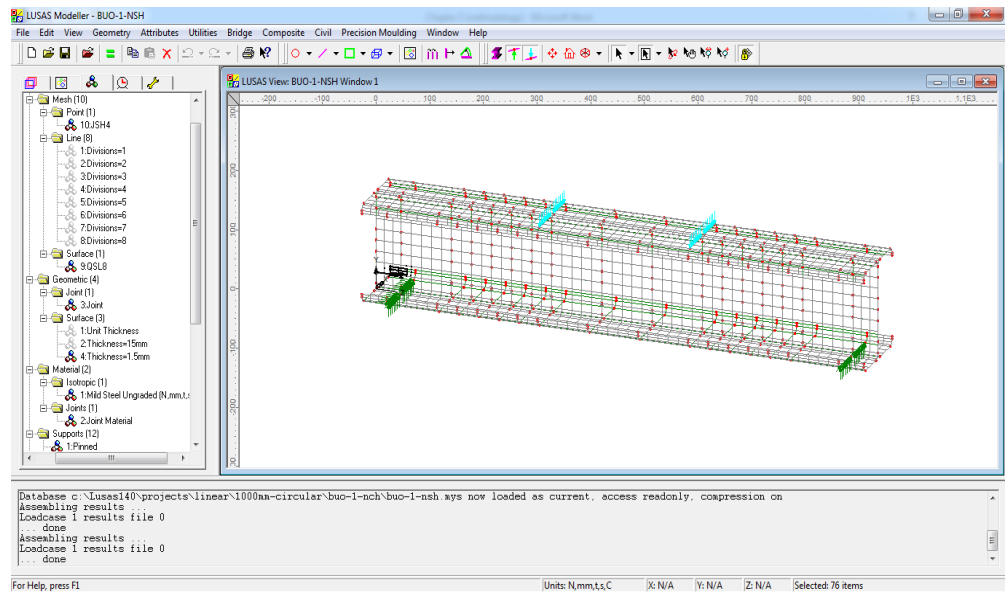


Figure 3.26 Completed model of BUO-1-NCH

CHAPTER 4

RESULTS AND DISCUSSION

4.1 Introduction

In this chapter, the result performed from the numerical analysis by using LUSAS software is discussed. From the result obtained, the several conditions of variety deformed shape and contour stress value of the built-up open model will be explained. The effect of different shapes and numbers of the opening with three perspective beam length was compared in this analysis. The maximum buckling load are calculated by eigenvalue analysis. The result and data analysis are presented on figures and tables for better understanding.

4.2 Result of Finite Element Analysis (FEA)

FEA of perforated built-up open CFS subjected to bending was conducted to carry out the linear analysis and linear buckling analysis (eigenvalue). The result are obtained by following the scope of study below:

- i. Different shapes of opening for each specimen
- ii. Number of openings set for each beam
- iii. Different perspective length of beam

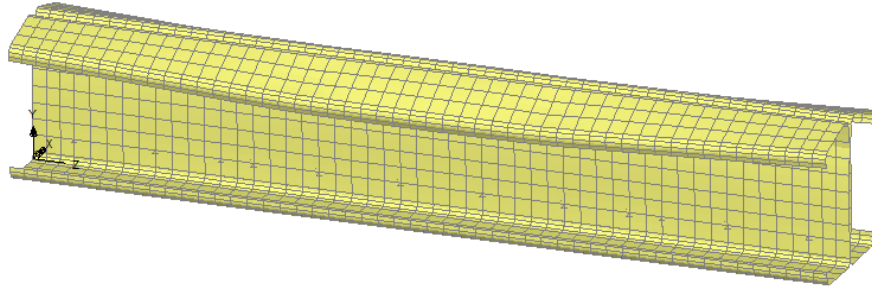
4.3 Linear Analysis

In linear analysis, the deformed shapes and contour stress with the maximum tension and compression stress value are determined. The result obtained are shown in figures and tabulated in table.

4.3.1 Deformed Mesh Square Opening Shapes

Figure 4.1 – 4.3 show the nine samples of the deformed shape of built-up open CFS beam for perspective length of 1000 mm, 1500 mm and 2000 mm span with and without square opening shape. In this analysis, the materials bodies of the specimens are deformed thus, deflected from the initial positions when the loads are applied. As stated by Malike and Abd Hamid (2012), it is the location where the specimens receive the largest load distribution from the loading.

From the observation, the specimen without openings created the highest strength than the specimen with openings. The specimen that having the highest number of square opening with a longest beam span undergoes the largest displacement compare to others. Due to three perspectives beam length, the longest span deflected more than the shortest one. By comparing the number of openings, built-up open CFS beams with four square openings is having a larger deformation compare to two square openings.



(a)

(b)

(c)

Figure 4.1 Deformed shape for (a) BUO-1-NSH, (b) BUO-1-2SH, (c) BUO-1-4SH

(a)

(b)

(c)

Figure 4.2 Deformed shape for (a) BUO-2-NSH, (b) BUO-2-2SH, (c) BUO-2-4SH

(a)

(b)

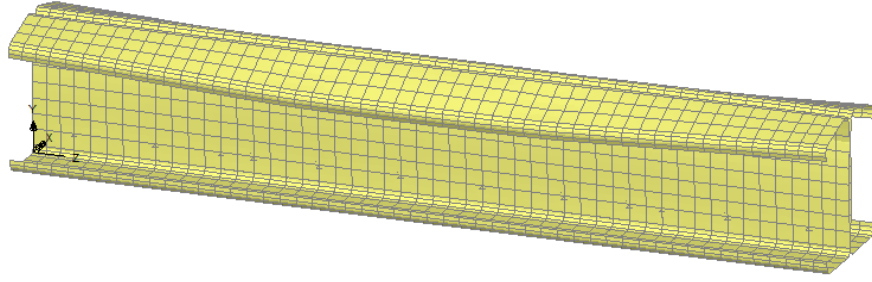
(c)

Figure 4.3 Deformed shape for (a) BUO-3-NSH, (b) BUO-3-2SH, (c) BUO-3-4SH

4.3.2 Deformed Mesh Circular Opening Shapes

Figure 4.4 – 4.6 show the deformed shape for perspective length of 1000 mm, 1500 mm and 2000 mm beams span with and without circular opening shape. In this analysis, generally, the deformations will be occur on the point where the loads are applied. As stated by Malike and Abd Hamid, (2012), it is the location where the specimens receives the largest load distribution from the loading. Thus, the specimens was experienced deflection from the initial condition.

The result are similar to the square opening where the specimens that having the highest number of circular opening with a longest beam span are undergoes the largest displacement compare to others. From the observation, the specimen without openings created the highest strength than the specimen with openings. Due to three perspectives beam length, the longest span deflected more than the shortest one. By comparing the number of openings, built-up open CFS beams with four circular openings is having a larger deformation compare to two circular openings.



(a)

(b)

(c)

Figure 4.4 Deformed shape for (a) BUO-1-NCH, (b) BUO-1-2CH, (c) BUO-1-4CH

(a)

(b)

(c)

Figure 4.5 Deformed shape for (a) BUO-2-NCH, (b) BUO-2-2CH, (c) BUO-2-4CH

(a)

(b)

(c)

Figure 4.6 Deformed shape for (a) BUO-3-NCH, (b) BUO-3-2CH, (c) BUO-3-4CH

4.3.3 Contour Stress Square Opening Shapes

Figure 4.7 – Figure 4.9 show the contour stress of the specimens with the maximum tension and compression stress value of the built-up open CFS beam due to different perspective length with different number of the square openings. From the stress figure, positive value indicate the CFS beam are under tension and the negative value show the CFS beam under compression. The location of the maximum tension is always located at the mid-span of the CFS beam while the maximum compression stress is located near to the support. It was found that all the specimens displayed a localized failure above the web hole when the ultimate load was reached. The results are experienced by Wang and Young (2015) about the research of beam tests of CFS built-up sections with web perforations. This indicates that the presence of holes would initiate the failure of a beam.

In Figure 4.7 which represent the specimens with 1000 mm beam length, the tension stress value increasing and the compression stress value decreasing when the number of square opening increases. While, in Figure 4.8 and Figure 4.9, for the specimens with 1500 mm beam and 2000 mm beam length, the tension stress value and compression stress value is fluctuated when the number of square opening increases but both value are lesser than the specimens with 1000 mm beam length. The maximum tension and compression value of the square opening specimens are illustrated in Table 4.1.

(a)

(b)

(c)

Figure 4.7 Contour stress for (a) BUO-1-NSH, (b) BUO-1-2SH, (c) BUO-1-4SH

(a)

(b)

Figure 4.8 Contour stress for (a) BUO-2-NSH, (b) BUO-2-2SH, (c) BUO-2-4SH

(c)

Figure 4.8 (Cont.)

(a)

Figure 4.9 Contour stress for (a) BUO-3-NSH, (b) BUO-3-2SH, (c) BUO-3-4SH

(b)

(c)

Figure 4.9 (Cont.)

4.3.4 Contour Stress Circular Opening Shapes

Figure 4.10 – Figure 4.12 shows the contour stress of the specimens with the maximum tension and compression stress value of the built-up open CFS beam due to different perspective length with different number of the circular openings. From the stress figure, positive value indicate the CFS beam are under tension and the negative value show the CFS beam under compression. The location of the maximum tension is always located at the mid-span of the CFS beam while the maximum compression stress is located near to the support. It was found that all the specimens displayed a localized failure above the web hole when the ultimate load was reached. The results are experienced by Wang and Young (2015) about the research of beam tests of CFS built-up sections with web perforations. This indicates that the presence of holes would initiate the failure of a beam.

In Figure 4.10 which represent the specimens with 1000 mm beam length, the tension stress value and the compression stress value decreasing when the number of circular opening increases. While, in Figure 4.11 and Figure 4.12, for the specimens with 1500 mm beam and 2000 mm beam length, the tension stress value and compression stress value is fluctuated when the number of circular opening increases but both values are lesser than the specimens with 1000 mm beam length. The maximum tension and compression value of the circular opening specimens are illustrated in Table 4.1.

(a)

(b)

(c)

Figure 4.10 Contour stress for (a) BUO-1-NCH, (b) BUO-1-2CH, (c) BUO-1-4CH

(a)

(b)

Figure 4.11 Contour stress for (a) BUO-2-NCH, (b) BUO-2-2CH, (c) BUO-2-4CH

(c)

Figure 4.11 (Cont.)

(a)

Figure 4.12 Contour stress for (a) BUO-3-NCH, (b) BUO-3-2CH, (c) BUO-3-4CH

(b)

(c)

Figure 4.12 (Cont.)

Table 4.1 Maximum Stress of CFS Beam

Opening	Stress (N/mm ²)			Stress (N/mm ²)			Stress (N/mm ²)		
	Models	Tension (10 ³)	Compression (10 ³)	Test 2: Two Holes	Tension (10 ³)	Compression (10 ³)	Test 3: Four Holes	Tension (10 ³)	Compression (10 ³)
Circular	BUO-1-NCH	14.96	5.39	BUO-1-2CH	11.00	3.21	BUO-1-4CH	11.02	3.20
	BUO-2-NCH	12.00	3.44	BUO-2-2CH	12.00	3.56	BUO-2-4CH	12.12	3.46
	BUO-3-NCH	12.94	3.09	BUO-3-2CH	12.93	3.08	BUO-3-4CH	12.92	3.08
Square	BUO-1-NSH	14.96	5.39	BUO-1-2SH	15.00	5.39	BUO-1-4SH	15.00	5.38
	BUO-2-NSH	12.00	3.44	BUO-2-2SH	12.07	3.44	BUO-2-4SH	12.13	3.44
	BUO-3-NSH	12.94	3.09	BUO-3-2SH	12.91	3.08	BUO-3-4SH	12.94	3.09

4.4 Linear Buckling Analysis (Eigenvalue)

The maximum buckling load that can be carry by the perforated built-up CFS beam before it fails is determined by linear buckling analysis. In linear buckling analysis, most of the specimens are buckled to the right when the loads act on it. The conditions of the supports caused the specimens to deflected and buckled up or change from the original shapes. They are facing a failure behaviour of local buckling and lateral torsional buckling. The deformed shapes are identified and represented in the figures. The maximum buckling load are calculated and tabulated in table.

4.4.1 Deformed Mesh Square Opening Shapes

Figure 4.13 – Figure 4.15 shows the deformed shapes from eigenvalue analysis for built-up open CFS beam with and without square perforations regarding to three different perspective length of beam. The result shows that the higher the number of square openings, the greater the deformations occurred. The longest the beam span, the critical the deformed shape of the specimens.

(a)

(b)

(c)

Figure 4.13 Deformed shapes of eigenvalue analysis for (a) BUO-1-NSH, (b) BUO-1-2SH, (c) BUO-1-4SH

(a)

(b)

(c)

Figure 4.14 Deformed shapes of eigenvalue analysis for (a) BUO-2-NSH, (b) BUO-2-2SH, (c) BUO-2-4SH

(a)

(b)

Figure 4.15 Deformed shapes of eigenvalue analysis for (a) BUO-3-NSH, (b) BUO-3-2SH, (c) BUO-3-4SH

(c)

Figure 4.15 (Cont.)

4.4.2 Deformed Mesh Circular Opening Shapes

Figure 4.16 – Figure 4.18 shows the deformed shapes from eigenvalue analysis for built-up open CFS beam with and without circular perforations regarding to three different perspective length of beam. The result shows that the higher the number of circular openings, the greater the deformations occurred. The longest the beam span, the critical the deformed shape of the specimens.

(a)

(b)

(c)

Figure 4.16 Deformed shapes of eigenvalue analysis for (a) BUO-1-NCH, (b) BUO-1-2CH, (c) BUO-1-4CH

(a)

(b)

(c)

Figure 4.17 Deformed shapes of eigenvalue analysis for (a) BUO-2-NCH, (b) BUO-2-2CH, (c) BUO-2-4CH

(a)

(b)

Figure 4.18 Deformed shapes of eigenvalue analysis for (a) BUO-3-NCH, (b) BUO-3-2CH, (c) BUO-3-4CH

(c)

Figure 4.18 (Cont.)

4.4.3 Contour Stress Square Opening Shapes (Eigenvalue)

Figure 4.19 – Figure 4.21 show the contour stress of the specimens with the maximum tension and compression stress value of the built-up open CFS beam due to different perspective length with different number of the square openings by using linear buckling analysis. From the stress figure, positive value indicate the CFS beam are under tension and the negative value show the CFS beam under compression. The location of the maximum tension is always located at the mid-span of the CFS beam while the maximum compression stress is located near to the support.

In Figure 4.19 – Figure 4.21, which represent the specimens with 1000 mm, 1500 mm and 2000 mm perspective beam length are show that the tension stress value and the compression stress value decreasing when the number of square opening increases. However, the eigenvalue load factor is decreases when the number of square opening increases. This is experienced by Ling et al. (2015) which they concluded that the web profile with small web opening show insignificant difference of the buckling moment. As the opening sizes greater, the buckling load capacity will decreases. Then, the buckling load is calculated by multiplying the concentrated load, 8000 N with the eigenvalue load factor. The maximum buckling load of the square opening specimens are illustrated in Table 4.2.

(a)

(b)

(c)

Figure 4.19 Contour stress of eigenvalue analysis for (a) BUO-1-NSH, (b) BUO-1-2SH,
(c) BUO-1-4SH

(a)

(b)

Figure 4.20 Contour stress of eigenvalue analysis for (a) BUO-2-NSH, (b) BUO-2-2SH,
(c) BUO-2-4SH

(c)

Figure 4.20 (Cont.)

(a)

Figure 4.21 Contour stress of eigenvalue analysis for (a) BUO-3-NSH, (b) BUO-3-2SH,
(c) BUO-3-4SH

(b)

(c)

Figure 4.21 (Cont.)

4.4.4 Contour Stress of Circular Opening Shapes (Eigenvalue)

Figure 4.22 – Figure 4.24 show the contour stress of the specimens with the maximum tension and compression stress value of the built-up open CFS beam due to different perspective length with different number of the circular openings by using linear buckling analysis. From the stress figure, positive value indicate the CFS beam are under tension and the negative value show the CFS beam under compression. The location of the maximum tension is always located at the mid-span of the CFS beam while the maximum compression stress is located near to the support.

In Figure 4.22 and Figure 4.24, which represent the specimens with 1000 mm and 2000 mm beam length are show that the tension stress value and the compression stress value decreasing when the number of circular opening increases. While, in Figure 4.23 that illustrate the specimens with 1500 mm beam length, the tension and compression stress value are fluctuated when the number of circular opening increases. However, the eigenvalue load factor is decreases when the number of circular opening increases. This is experienced by Ling et al. (2015) which they concluded that the web profile with small web opening show insignificant difference of the buckling moment. As the opening sizes greater, the buckling load capacity will decreases. Then, the buckling load is calculated by multiplying the concentrated load, 8000 N with the eigenvalue load factor. The maximum buckling load of the circular opening specimens are illustrated in Table 4.2.

(a)

(b)

(c)

Figure 4.22 Contour stress of eigenvalue analysis for (a) BUO-1-NCH, (b) BUO-1-2CH, (c) BUO-1-4CH

(a)

(b)

Figure 4.23 Contour stress of eigenvalue analysis for (a) BUO-2-NCH, (b) BUO-2-2CH, (c) BUO-2-4CH

(c)

Figure 4.23 (Cont.)

(a)

Figure 4.24 Contour stress of eigenvalue analysis for (a) BUO-3-NCH, (b) BUO-3-2CH, (c) BUO-3-4CH

(b)

(c)

Figure 4.24 (Cont.)

Table 4.2 Linear Buckling Analysis

	Models	Eigenvalue			Eigenvalue			Eigenvalue		
		Test 1: No Holes	Load Factor (10^{-1})	Buckling Load (kN)	Test 2: Two Holes	Load Factor (10^{-1})	Buckling Load (kN)	Test 3: Four Holes	Load Factor (10^{-1})	Buckling Load (kN)
Circular	BUO-1-NCH	0.3192	2.55	BUO-1-2CH	0.4440	3.55	BUO-1-4CH	0.4414	3.53	
	BUO-2-NCH	0.4480	3.58	BUO-2-2CH	0.4491	3.59	BUO-2-4CH	0.4413	3.53	
	BUO-3-NCH	0.4703	3.76	BUO-3-2CH	0.4673	3.74	BUO-3-4CH	0.4630	3.70	
Square	BUO-1-NSH	0.3192	2.55	BUO-1-2SH	0.3170	2.54	BUO-1-4SH	0.3140	2.51	
	BUO-2-NSH	0.4480	3.58	BUO-2-2SH	0.4455	3.56	BUO-2-4SH	0.4398	3.52	
	BUO-3-NSH	0.4703	3.76	BUO-3-2SH	0.4654	3.72	BUO-3-4SH	0.4549	3.64	

CHAPTER 5

CONCLUSION

5.1 Introduction

The deformed shape and maximum stress are obtained from the numerical analysis by using finite element modelling of LUSAS software version 14.0. The selected attribute mesh, geometry, materials, support and loading conditions in modelling process have been described in this study. The modelling was validated by following the parametric study in this research. The linear analysis and linear buckling analysis has been done to analyse the deformed shapes, displacements, maximum stresses and maximum eigenvalue buckling load. From the analysis, the failure modes of the specimens are identified and the effect of different shapes and number of opening to perforated built-up open CFS beams are determined. The maximum stresses and maximum buckling load are calculated and specifically described in detail.

5.2 Conclusion

From the numerical simulations of finite element analysis on perforated built-up open CFS beam, the following conclusions has been presented:

- i. From the finite element analysis, the perforations aspect is effect the linear analysis and linear buckling analysis of built-up open CFS beam. From the linear analysis, it illustrate that the built-up open CFS section with square openings have the higher stress value than circular openings. By comparing the number of openings, built-up open CFS beams with four openings is having a larger deformation compare to two openings.
- ii. The perforated built-up open CFS beam sections with perspective length of 1000 mm shows the highest tension stress compared to others length. It also shows when the span of beam is longest, the compression stress is lowest. The highest number of circular openings with shortest perspective span shows the lowest tension stress than others while, the highest number of square opening with longest perspective span shows the lowest tension stress than others.
- iii. From linear buckling analysis result, the maximum value of buckling load for CFS beam without perforations is lowest compare to CFS beam with perforations. When the number of opening increases, the value of buckling load is decreases. So, the deformation of buckling criteria also changes. The shortest perspective span created the lowest value of the buckling load compared to others. Eigenvalue result also shows that the built-up CFS beam section with circular opening recorded the higher buckling load than the square perforation.

REFERENCES

- Altan, M. F. and Kartal, M. E. 2009. Investigation of Buckling Behavior of Laminated Reinforced Concrete Plates with Central Rectangular Hole Using Finite Element Method. *Material & Design*. 30(6): 2243-2249.
- Degtyarev, V. V. and Degtyareva, N. V. 2018. Numerical simulations on cold-formed steel channels with longitudinally stiffed slotted webs in shear. *Thin-Walled Structures*. 129: 429-456.
- Fratamico, T. C., Torabian, S., Zhao, X., Rasmussen, K. J. R. and Schafer, B. W. 2018. Experiments on the global buckling and collapse of built-up cold-formed steel columns. *Journal of Constructional Steel Research*. 144: 65-80.
- Fratamico, D. C., Torabian, S., Zhao, X., Rasmussen, K. J. R. and Schafer, B. W. 2018. Numerical studies on the composite action in sheated and bare built-up cold-formed steel columns. *Thin-Walled Structures*. 127: 290-305.
- Gilbert, B. P., Timothee, J., Savoyat, M. and Teh, L. H. 2012. Self-Shape Optimisation Application: Optimisation of Cold-Formed Steel Columns. *Thin-Walled Structures*. 60: 173-184.
- Kim, J. H., Lee, M. G., Kim, D., Matlock, D. K. and Wagoner, R. H. 2010. Hole-expansion formability of Dual-Phase Steels using Representative Volume Element Approach with Boundary-Smoothing Technique. *Materials Science and Engineering*. 527(27-28): 7353-7363.
- Kulatunga, M. and Macdonald, M. 2013. Investigation of cold-formed steel structural members with perforations of different arrangements subjected to compression loading. *Thin-Walled Structures*. 67: 78-87.
- Laboube, R. A. and Yu, W. W. 2010. Recent research and developments in cold-formed steel framing. *Thin-Walled Structures*. 32(1-3): 19-39.

Ling, J. Y., Kong, S. L. and De'nan, F. 2015. Numerical study of buckling behavior of cold-formed c-channel steel purlin with perforation. *Procedia Engineering*. 125: 1135-1141.

LUSAS Finite Element Analysis (FEA) Software. United Kingdom. 2009.

Malike, S. S. and Abd Hamid, K. J. 2012. Direct Strength Method (DSM) for cold-formed steel column with holes. *Procedia Civil Engineering*.

Pham, C. H. and Hancock, G. J. 2010. Numerical simulation of high strength cold-formed purlins in combined bending and shear. *Journal of Constructional Steel Research*. 66(10): 1205-1217.

Seo, J. K. and Mahendran, M. 2012. Member moment capacities of mono-symmetric LiteSteel Beam floor joists with web openings. *J. Constr. Steel Res.* 70: 153-166.

Seo, J. K., Mahendran, M. and Paik, J. K. 2011. Numerical method for predicting the elastic lateral torsional buckling moment of a mono-symmetric beam with web openings. *Thin-Wall Structure*. 49(6): 713-723.

Sivakumaran, K. S., Ng, M. Y. and Fox, S. R. 2006. Flexural strength of cold-formed steel joists with reinforced web openings. *Can. J. Civil Eng.* 33(9): 1195-1208.

Vieira Jr, L. C., Malite, M. and Schafer, B. W. 2008. Numerical analysis of cold-formed steel purlin-sheeting systems. *Thin-Walled Structures*.

Vraný, T. 2006. Effect of loading on the rotational restraint of cold-formed purlins. *Thin-Walled Structures*. 44(12): 1287-1292.

Wang, L. and Young, B. 2017. Design of cold-formed steel built-up sections with web perforations subjected to bending. *Thin-Walled Structures*. 120: 458-469.

Wang, L. and Young, B. 2015. Beam tests of cold-formed steel build-up sections with web perforations. *Journal of Constructional Steel Research*. 115: 18-33.

- Wang, H. and Zhang, Y. 2009. Experimental and numerical investigation on cold-formed steel C-section flexural members. *Journal of Constructional Steel Research*. 65(5): 1225-1235.
- Yang, J. and Liu, Q. 2012. Sleeve connections of cold-formed steel sigma purlins. *Engineering Structures*. 43: 245-258.
- Ye, J., Hajirasouliha, I., Becque, J. and Pilakoutas, K. 2016. Development of more efficient cold-formed steel channel sections in bending. *Thin-Walled Structures*. 101: 1-13.
- Yuan, W. B., Yu, N. T. and Li, L. Y. 2017. Distortional buckling of perforated cold-formed steel channel-section beams with circular holes in web. *International Journal of Mechanical Sciences*. 126: 255-260.
- Zhang, J. H. and Young, B. 2015. Numerical investigation and design of cold-formed steel built-up open section columns with longitudinal stiffeners. *Thin-Walled Structures*. 89: 178-191.